

# $^{151}\text{Eu}$ hyperfine fields, isomer shifts and moments in Eu-based $\text{EuT}_2\text{X}_2$ intermetallic compounds

D. H. Ryan · J. M. Cadogan

© Springer Science+Business Media Dordrecht 2013

**Abstract** The closed-shell, well-screened europium moment should make its compounds an easy and robust system in which to study the correlation between the local moment and the observed hyperfine field ( $B_{\text{hf}}$ ). Having explored why one might expect  $B_{\text{hf}}$  to provide a reasonable measure of the local moment, and why the isomer shift ( $\delta$ ) might allow for a first-order correction to include the effects of the local chemical environment, we proceed with an analysis of the extensive  $^{151}\text{Eu}$  Mössbauer data on the  $\text{EuT}_2\text{X}_2$  compound family. We find that while in some limited cases a useful correlation may exist, in general there are far too many as yet unknown contributions to  $B_{\text{hf}}$  for it to provide a meaningful estimate of the moment.

**Keywords** Europium compounds · Mössbauer spectroscopy · Hyperfine fields · Moments · Magnetic order

## 1 Introduction

The almost perfect complementarity between the local information derived from Mössbauer spectroscopy and the long-range structural data provided by neutron diffraction makes the two techniques invaluable in the study of magnetic ordering.

---

Proceedings of the 32nd International Conference on the Applications of the Mössbauer Effect (ICAME 2013) held in Opatija, Croatia, 1–6 September 2013.

D. H. Ryan (✉)  
Department of Physics and Centre for the Physics of Materials, McGill University,  
3600 University St., Montreal, QC, H3A2T8, Canada  
e-mail: dhryan@physics.mcgill.ca

J. M. Cadogan  
School of Physical, Environmental and Mathematical Sciences,  
UNSW Canberra at the Australian Defence Force Academy,  
Canberra, BC 2610, Australia  
e-mail: s.cadogan@adfa.edu.au

The appearance of a magnetic hyperfine field ( $B_{\text{hf}}$ ) in a Mössbauer spectrum almost invariably signals the development of magnetic order of some form (the spin-spin correlations may only be short ranged, or even short lived, but they have to exist for the field to be observed), while the appearance of magnetic scattering in a neutron diffraction pattern signals the development of long range magnetic order. Where the effects of an electric field gradient (efg) are observed, and the local point symmetry of the site occupied by the Mössbauer probe is useful (too high, e.g. cubic, yields no efg, too low, e.g. monoclinic, and the mapping onto the crystallographic reference frame is difficult to establish [1]) then the direction of the magnetic ordering can often be determined, providing independent confirmation of neutron diffraction analysis. This is especially useful where spin reorientation events occur as, even without knowing the direct efg→crystal axis mappings, a rotation can be observed and often its magnitude can be determined. Where the Mössbauer probe occupies distinct crystallographic sites that exhibit different ordering transitions, it is possible to observe this behaviour unambiguously in the Mössbauer spectrum [2] and greatly assist the analysis of neutron diffraction data. Finally, neutron diffraction cannot be used to distinguish between with a reduced moment at a given site, from ordering in which only part of the sample orders but with a much larger moment, whereas this is relatively straightforward using Mössbauer spectroscopy.

Unfortunately, there is one key piece of information that cannot reliably be extracted from a Mössbauer spectrum: *the moment*. Despite extensive experimental and theoretical work, and no little wishful thinking, in most cases there are just too many unknown contributions for the local moment to be extracted from a Mössbauer spectrum with any real confidence. However, as we will show, with some care, and with complementary information from neutron diffraction, useful insights are still possible.

We will look briefly at the two most popular Mössbauer isotopes ( $^{57}\text{Fe}$  and  $^{119}\text{Sn}$ ) before moving on to our primary interest,  $^{151}\text{Eu}$ .

## 2 Contributions to the hyperfine field

In the absence of an externally applied magnetic field, the hyperfine field,  $B_{\text{hf}}$ , at a Mössbauer nucleus can be written as the vectorial sum of four contributions:

$$\vec{B}_{\text{hf}} = \vec{B}_{\text{n}} + \vec{B}_{\text{d}} + \vec{B}_{\text{orb}} + \vec{B}_{\text{c}} \quad (1)$$

where  $B_{\text{n}}$  includes the effects of surrounding (typically first-neighbour) moments;  $B_{\text{d}}$  and  $B_{\text{orb}}$  represent dipolar and orbital contributions from non-core (non s-like) electrons on the atom, typically small (few Tesla) in iron [3–6]; and  $B_{\text{c}}$  is the core polarisation or Fermi contact term, which results from exchange polarisation of the s-electrons (the only ones having any overlap with the nucleus) by the moment-carrying (d- or f-) electrons. This last term reflects an imbalance between spin-up ( $\uparrow$ ) and spin-down ( $\downarrow$ ) electrons in the nuclear volume ( $\rho(0)$ ):

$$B_{\text{c}} = a' \sum [\rho_i^{\uparrow}(0) - \rho_i^{\downarrow}(0)] \quad (2)$$

where  $a'$  is a proportionality constant.  $B_{\text{c}}$  is often subdivided into two terms:

$$B_{\text{c}} = B_{\text{cp}} + B_{\text{cep}} \quad (3)$$

with  $B_{cp}$  representing the field due to polarisation of the truly “core” electrons (1s, 2s, 3s) and  $B_{cep}$  reflecting the contributions of the valence and conduction band electrons (4s, 3d, 4p,...). The reason for this decomposition is that only  $B_{cp}$  is truly proportional to the 3d moment [3] so  $B_c$  can be written:

$$B_c = a \mu_{3d} + b [\rho^\uparrow(0) - \rho^\downarrow(0)] \quad (4)$$

where  $a$  and  $b$  are scale factors and  $\rho(0)$  is the *total* band electron contact density.

Herein lies the problem. Changing the chemistry (local environment, bonding, etc.) impacts the conduction and valence electron densities, affecting both  $\rho(0)$ , as the electron density changes, and also  $b$  as this density change will modify the screening within that atom and so change the effectiveness with which the spin polarisation reaches the nucleus. By the same token,  $a$  may be expected to change as the core electron density (1s, 2s, 3s) is affected by the environment. Indeed  $B_c$  has been reported to scale with the isomer shift in Fe/V sandwiches [6] and the scale factor in Fe-Cr clusters may even change *sign* depending on the local coordination [7]. Finally, even within a single material, the scaling between the moment and observed hyperfine field can be temperature dependent [8].

The problems with seeking a simple conversion factor between the local moment and  $B_{hf}$  in iron-based systems have been reviewed extensively in a recent article by Dubiel [9]. Measured scale factors vary wildly between systems, affected by chemistry and even by local ordering for the same composition. In some cases the variation within a single system may exceed a factor of ten. In most disciplines, an uncertainty in the exponent is considered “wrong”.

### 3 An example with no local contribution: <sup>119</sup>Sn

While tin lacks a local moment, the <sup>119</sup>Sn Mössbauer transition is relatively easy to work with, it provides good resolution, and it has a large quadrupole interaction making it possible to determine the orientation of  $B_{hf}$  in the efg axis system. This can be extremely useful in conjunction with neutron diffraction data. While the absence of a local moment puts <sup>119</sup>Sn Mössbauer spectroscopy somewhat outside the current topic, it is included here as it provides a very clean demonstration of an important complicating factor in any attempt to determine a moment from  $B_{hf}$ . The possible presence of an orbital contribution,  $B_{orb}$ , means that the hyperfine field can be affected by the positions and orientations of neighbouring moments and not just by their magnitude [10, 11].

The simplest way to see this effect is to study systems in which the magnetic order reorients by 90°, either spontaneously or in response to an externally applied field. The hexagonal RMn<sub>6</sub>Sn<sub>6</sub> system (doped with Ga or In to promote ferromagnetic ordering rather than the more complex antiferromagnetic or helimagnetic ordering that occurs in the parent compounds) provides an ideal demonstration of the anisotropic contributions to  $B_{hf}$  [12]. The tin occupies three readily distinguishable sites in the structure with quite different quadrupole and magnetic interactions. For each tin site, the point symmetry forces the asymmetry parameter,  $\eta$ , to be zero and places the principal axis of the efg tensor  $V_{zz}$  along one (indeterminate) of the crystal axes. Remarkably, the three sites exhibit quite different responses to a 90° rotation of the magnetic ordering direction. For example, in ErMn<sub>6</sub>Sn<sub>5.89</sub>Ga<sub>0.11</sub>,

nothing happens at the Sn-2c site,  $B_{\text{hf}}$  decreases by 10 % (about 3 T) at the Sn-2d site, while at the Sn-2e site  $B_{\text{hf}}$  increases by over 30 % (about 5 T) [12, 13]. These changes are large enough that the field sequence is affected:  $2d > 2c > 2e$  for order along  $c$ , to  $2c > 2d > 2e$  for basal plane order, affecting early site assignments based on simple neighbour counts and distances.

Despite the limitations on absolute field scales,  $^{119}\text{Sn}$  Mössbauer spectroscopy can be very effective in identifying the *form* of the magnetic order in complex systems by using the *distribution* of  $B_{\text{hf}}$  observed at the tin sites [14]. Simple ferromagnetic or antiferromagnetic structures yield a single tin site with a unique field. More complex structures can lead to magnetically inequivalent tin sites, as for example in the  $\text{RFe}_6\text{Sn}_6$  system where the transferred field from the Fe moments lead to zero-field and large field tin sites with an area ratio of 2:1 [15]. Where the ordering is modulated or incommensurate, more complex, but characteristic, field distributions are observed [14]. In particular, even weakly incommensurate structures (i.e. magnetic structures with periods that are almost rational multiples of lattice parameters) lead to profoundly different distributions of hyperfine fields from those seen in long-period commensurate structures [14].

## 4 Hyperfine fields in europium compounds

### 4.1 Background

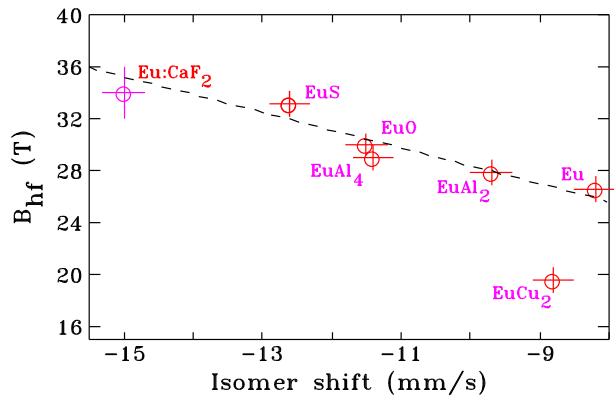
Europium might be expected to be simpler than either iron or tin as it has a large ( $7 \mu_B$ ) local moment (in  $\text{Eu}^{2+}$ ) associated with a half-filled  $4f$  shell. This moment should be the dominant source of the observed hyperfine field, so the effects of neighbours will be limited. The  $L = 0$ ,  $^8S_{7/2}$  ground state has no orbital component, so the anisotropic contributions that cause so much trouble with  $^{119}\text{Sn}$ , should be small. Finally, the  $4f$  shell is reasonably well shielded, so the moment is largely unaffected by the chemical environment or crystal fields. In most cases therefore, a full  $7 \mu_B$  should be present in the ordered state, and one might expect a fairly narrow range of hyperfine fields in magnetically ordered  $\text{Eu}^{2+}$  compounds. This is not the case.

The europium system is an excellent place to study the origins of this failure to exhibit simple behaviour.  $^{151}\text{Eu}$  Mössbauer spectroscopy is relatively easy. The resonant isotope is abundant (48 % of natural europium—indeed the other stable isotope,  $^{153}\text{Eu}$ , also exhibits a usable resonance, but at 48 hrs the short half-life of the parent makes it inconvenient to work with and the 103 keV  $\gamma$  demands cold-source techniques to observe a signal) the  $\gamma$  energy is a convenient 21.5 keV making observations well above ambient temperatures possible, and the 90 year half-life of the parent  $^{151}\text{Sm}$  makes the source extremely stable, although effective activities tend to be very low. The spectra are generally well resolved with large hyperfine fields and isomer shifts, but a poorly resolved quadrupole interaction. The range of isomer shifts is remarkable, going from  $-15$  mm/s ( $\text{Eu}^{2+}$ ) to  $+5$  mm/s ( $\text{Eu}^{3+}$ ) [16], making the technique very sensitive to changes in  $\rho(0)$ , so the impact of chemistry on the scale factors in (4) is accessible to investigation.

If we include the effects of neighbouring moments in (3), our expression for the hyperfine field is [17]:

$$B_{\text{hf}} = B_{\text{cp}} + B_{\text{cep}} + B_{\text{n}} \quad (5)$$

**Fig. 1** Plot of hyperfine field ( $B_{\text{hf}}$ ) vs. isomer shift ( $\delta$ ) for a variety of  $\text{Eu}^{2+}$  compounds taken from the compilation by Wickman et al. [18]. The dashed line is a linear fit (omitting  $\text{EuCu}_2$ ) with a slope of  $-1.4(3)$  T/(mm/s)



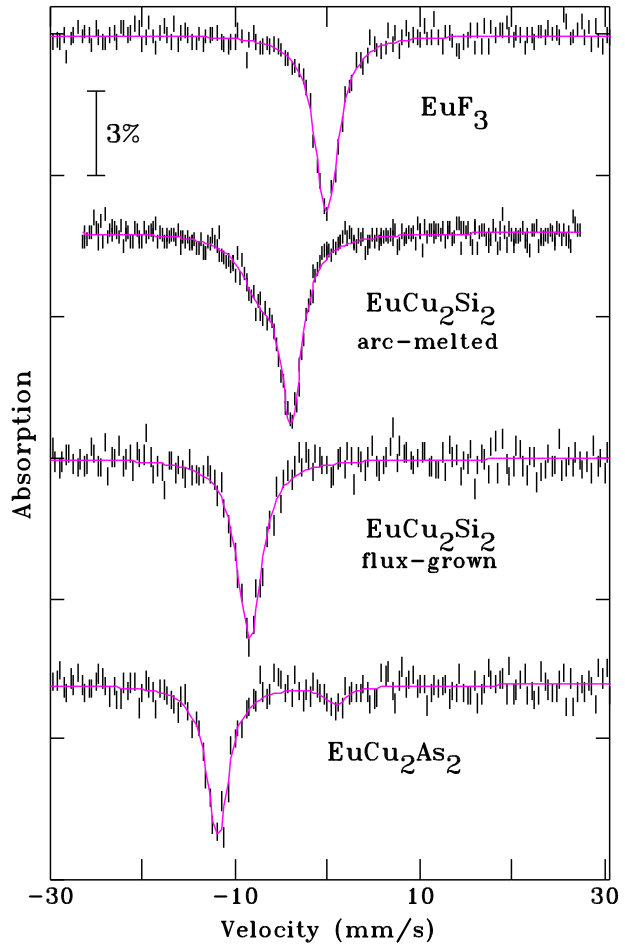
where the components have the same meanings given earlier. Working with two iso-valent substitutions (Ba and Yb) Hüfner and Wernick [19] measured  $B_{\text{hf}}$  in  $\text{Eu}_{1-x}\text{Yb}_x$  and  $\text{Eu}_{1-x}\text{Ba}_x$ , and assuming a core polarisation  $B_{\text{cp}}$  of  $-34(2)$  T [20, 21], estimated  $B_{\text{cep}}$  to be  $+19(2)$  T in their systems. Applying this to europium metal gave them an estimate of  $-11.5(2.0)$  T for  $B_{\text{n}}$  in the pure metal, so that all three terms are of comparable magnitude. In a later study, van Steenwijk et al. [22] looked at a series of hexagonal  $\text{CaCu}_5$ -type  $\text{EuT}_5$  ferromagnetic compounds ( $\text{T} = \text{Cu}, \text{Zn}, \text{Ag}, \text{Au}$ ) diluted with calcium or lanthanum, and found  $B_{\text{n}}$  for their systems to be consistent with zero ( $< 0.5$  T), showing that the Eu–Eu distance and probably the band structure of the host system play significant roles in setting  $B_{\text{n}}$ . While this procedure may be expected to work quite well at fixed electronic structure and density, the scale factors  $a$  and  $b$  in (4) will depend on total electron density within the nuclear volume ( $\rho(0)$ ), and this is strongly affected by bonding and chemistry.

An early compilation by Wickman et al. [18] shown in Fig. 1 gives an idea of the scale of the effect.  $B_{\text{hf}}$  and  $\delta$  (the isomer shift) adopt a wide range of values and are very strongly correlated. This is because, in principle, they reflect two related but distinct quantities.  $\delta$  provides information on the *total* density of electrons in the nuclear volume ( $\rho(0)$ ), while for a fixed magnetic environment,  $B_{\text{hf}}$  depends on the imbalance between spin-up and spin-down electrons in the same nuclear volume, i.e. ( $\rho^{\uparrow}(0) - \rho^{\downarrow}(0)$ ). While drawing attention to the correlation, the data in Fig. 1 are derived from a rather diverse set of materials: ionic compounds ( $\text{EuF}_2$ ,  $\text{EuO}$ ), some intermetallic compounds (e.g.  $\text{EuAl}_4$ ) and the pure element ( $\text{Eu}$ ). The chemistries of Al, S, F are quite different. Furthermore, even this small set has an outlier ( $\text{EuCu}_2$ ). We therefore turned to a more consistent environment in which to investigate the correlations between  $B_{\text{hf}}$  and  $\delta$ .

#### 4.2 Using the $\text{EuT}_2\text{X}_2$ compounds

The  $\text{EuT}_2\text{X}_2$  ( $\text{T} =$  transition metal e.g. Cr, Mn, Fe, Cu;  $\text{X} =$  group IV or V element e.g. Si, Ge, Sn, P, As, Sb) compound family form a very large group of materials that, for the most part, adopt the body centred tetragonal  $\text{ThCr}_2\text{Si}_2$  structure ( $I4/mmm$ ) with a unique crystallographic site for each constituent element. The europium atoms form sheets in the  $ab$ -plane that are separated along  $c$  by the  $\text{T}_2\text{X}_2$  layers. In many cases the compounds order antiferromagnetically with the Eu moments forming

**Fig. 2** Some typical ambient temperature paramagnetic  $^{151}\text{Eu}$  Mössbauer spectra showing the progression of isomer shifts.  $\text{Eu}^{3+}$  in  $\text{EuF}_3$  has an isomer shift close to zero. Arc-melted  $\text{EuCu}_2\text{Si}_2$  is intervalent with two components evident, both of which show more negative shifts than  $\text{EuF}_3$ , while flux-grown single-crystal  $\text{EuCu}_2\text{Si}_2$  is fully divalent.  $\text{EuCu}_2\text{As}_2$  exhibits a close to extremal isomer shift for divalent intermetallic compounds. The additional feature near 0 mm/s is due to  $\text{Eu}_2\text{O}_3$



ferromagnetic sheets that are coupled antiferromagnetically along  $c$ . With a constant structure but broadly adjustable chemistry the  $\text{EuT}_2\text{X}_2$  system exhibits a surprising diversity of behaviour and so provides an excellent testing ground.

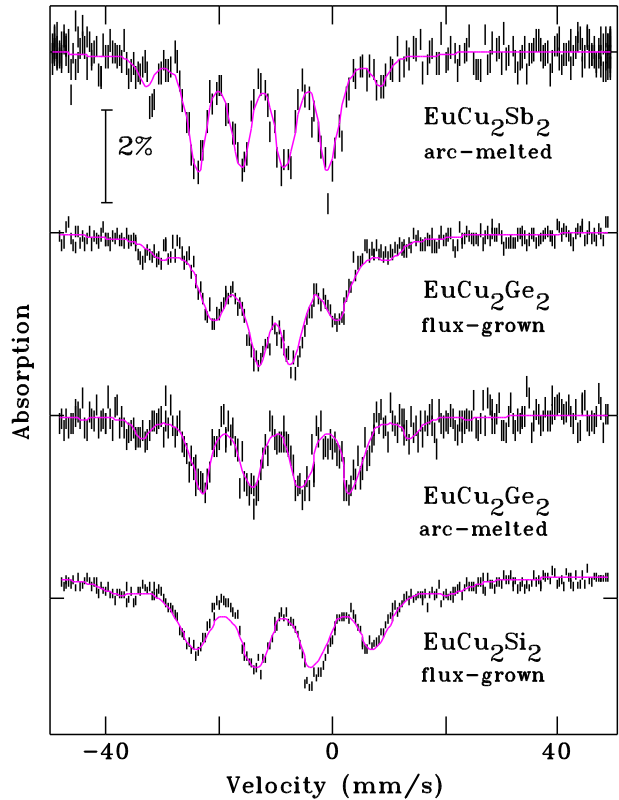
The first surprise is that the europium is not consistently divalent or trivalent, indeed,  $\text{EuCu}_2\text{Si}_2$  is probably the first intervalent europium compound identified [23], and the detailed behaviour is somewhat sample dependent. As can be seen in Fig. 2, the  $^{151}\text{Eu}$  Mössbauer spectrum for our arc-melted sample has two components. About 30 % of the area is associated with a broad component at  $-7.3(2)\text{mm/s}$ , rather positive for  $\text{Eu}^{2+}$ , while the remainder is associated with a sharp component with an isomer shift of  $-3.94(4)\text{mm/s}$ , inconsistent with either  $\text{Eu}^{3+}$  or  $\text{Eu}^{2+}$ . Furthermore, this line moves to more negative isomer shifts as the temperature increases [23], suggesting a progressive shift in the europium valence towards  $\text{Eu}^{2+}$ . This behaviour has been interpreted in terms of interconfigurational fluctuations [24, 25] and the  $\text{Eu}^{3+} \rightarrow \text{Eu}^{2+}$  transformation can also be driven by an externally applied field [26]. Many members of the  $\text{EuT}_2\text{Si}_2$  series exhibit similar behaviour.

Remarkably, the same material,  $\text{EuCu}_2\text{Si}_2$ , grown as single crystals from an indium flux adopts the same structure, with a slightly expanded lattice, and fully divalent europium [27]. A room temperature spectrum of flux-grown  $\text{EuCu}_2\text{Si}_2$  is shown in Fig. 2. The more negative isomer shift is clear, and is essentially independent of temperature [28]. Initial susceptibility measurements identified an antiferromagnetic transition at 10 K [27], however  $^{151}\text{Eu}$  Mössbauer work has been interpreted as showing that the ordering is spin-glass-like [29]. More recent neutron diffraction measurements confirmed that long-ranged antiferromagnetic order does indeed occur (Rowan-Weetaluktuk et al. 2014, unpublished).

The general variability of  $\text{EuCu}_2\text{Si}_2$ , and the confusion over the precise nature of the magnetic ordering in the flux-grown  $\text{EuCu}_2\text{Si}_2$  brings us to a significant limitation. In trying to understand how the isomer shift, hyperfine field and moment are related, it is essential that we have reliable values for all three, and indeed, also know the magnetic structure so that some allowance for the neighbour contribution,  $B_n$ , can be made. The Mössbauer parameters are generally easy to obtain with reasonable confidence, however, the moments and magnetic structures are more challenging. The thermal neutron absorption cross section of natural europium at 4530 b, is the third largest of all of the elements (after Gd and Sm, and ahead of Cd that is commonly used for neutron shielding) and gives it a  $1/e$  absorption depth of  $\sim 80$   $\mu\text{m}$ , making conventional approaches impractical. As a result, few magnetic structures have been measured, and most moment estimates come from fitting high temperature susceptibility data to a Curie-Weiss law and arguing for a full  $7 \mu_B$   $\text{Eu}^{2+}$  moment by observing the expected  $p_{\text{eff}}$  of  $7.94 \mu_B$ , although  $p_{\text{eff}}$  may be quite different (e.g.  $6.7(1) \mu_B$  in both  $\text{EuAu}_2\text{Si}_2$  and  $\text{GdAu}_2\text{Si}_2$  [30]), adding confusion rather than enlightenment.

Common approaches to the high neutron absorption problem are to use short wavelength (“hot”) neutrons, or to replace the natural europium with the less absorbing  $^{153}\text{Eu}$ . While hot neutrons have been used to great effect, with magnetic structures being determined for  $\text{EuCo}_2\text{P}_2$  [31] and  $\text{EuFe}_2\text{As}_2$  [32] for example, the short wavelengths (typically 0.5–0.8 Å) push all of the Bragg peaks down to low angles, and if the magnetic ordering involves a long-period structure, the fundamental peaks may be lost in the direct beam. Isotope replacement permits the use of longer wavelengths, but brings its own problems. While a conventional instrument may be used, the samples tend to be small due to the cost of the isotope, and this leads to potential difficulties with sample preparation and reproducibility, especially in the  $\text{EuT}_2\text{X}_2$  system where we have already seen significant variability between nominally identical samples.  $\text{EuMn}_2\text{Ge}_2$  is a case in point.  $^{151}\text{Eu}$  Mössbauer spectroscopy clearly showed the europium in  $\text{EuMn}_2\text{Ge}_2$  to be divalent, ordering at about 10 K [33, 34], while susceptibility and  $^{57}\text{Fe}$  Mössbauer spectroscopy showed that the manganese orders at 302 K [34]. However, a neutron diffraction study of a  $\sim 0.5$  g sample of  $\text{EuMn}_2\text{Ge}_2$  prepared using  $^{153}\text{Eu}$  [35], placed the ordering of the manganese at 667(9) K (extrapolated from their upper measuring limit of 623 K) and failed to find any evidence for ordering of the europium down to 1.8 K. As the sample contained no  $^{151}\text{Eu}$  by design, and was too small for  $^{153}\text{Eu}$  Mössbauer spectroscopy, it was not possible to independently confirm the valence or ordering of the europium in this sample.

**Fig. 3**  $^{151}\text{Eu}$  Mössbauer spectra for magnetically ordered  $\text{Eu}^{2+}$  intermetallic compounds of the form  $\text{EuT}_2\text{X}_2$ .  $B_{\text{hf}}$  increases from top to bottom, although the europium moment does not change. In addition, for flux-grown  $\text{EuCu}_2\text{Ge}_2$  and  $\text{EuCu}_2\text{Si}_2$ , the central lines are clearly lower than the two either side of them, reflecting the presence of magnetic relaxation. Spectra were measured at 5 K, except for  $\text{EuCu}_2\text{Sb}_2$  which was measured at 1.8 K



We recently developed a large-area flat-plate technique that allows us to work with highly absorbing materials without resorting to isotopic substitution [36], and have even used it to study Gd-based materials such as  $\text{Gd}_5(\text{Ge}, \text{Si})_4$  [37] at a long thermal wavelength of 2.37 Å. We were able to confirm that  $\text{EuCu}_2\text{P}_2$  is a canted ferromagnet [38], and have recently revisited the  $\text{EuMn}_2\text{Ge}_2$  problem, starting with a conventionally prepared 3 g arc-melted ingot. We found that the europium is indeed divalent, and both  $^{151}\text{Eu}$  Mössbauer spectroscopy and neutron diffraction, carried out on pieces of the original ingot, show that the europium orders at 10 K (Ryan et al. 2014, unpublished). We also confirmed that the manganese ordering temperature is 710 K, well above the original 302 K [34], but reasonably consistent with the extrapolation based on earlier neutron diffraction work [35]. As more europium-based systems are more fully characterised, the database of hyperfine fields, moments and magnetic structures will become more extensive and reliable, making a more thorough analysis of the relationships possible.

The  $^{151}\text{Eu}$  Mössbauer spectra of some  $\text{EuT}_2\text{X}_2$  samples taken at 5 K shown in Fig. 3 reveal one last complication. While the spectra for  $\text{EuCu}_2\text{Sb}_2$  and arc-melted  $\text{EuCu}_2\text{Ge}_2$  exhibit a conventional form with the central four lines (each is actually formed from three closely overlapping lines) having approximately the same

intensity, the spectra for the two flux-grown samples are quite different, with the central pair being visibly deeper than the lines either side of them. This form is characteristic of dynamics—moment fluctuations on the timescale of the Mössbauer event. Flux-grown  $\text{EuCu}_2\text{Ge}_2$  was originally identified as an antiferromagnet with two transitions at 9 K and 4 K [39, 40], while the presence of dynamics emerged later from a  $^{151}\text{Eu}$  Mössbauer study [41]. The assignment of the 4 K transition is based on a broad feature in susceptibility and has not been confirmed by either Mössbauer spectroscopy [41] (Ryan et al. 2014, unpublished) or neutron diffraction (Ryan et al. 2014, unpublished), and is likely an artefact. Similarly, fluctuations in the  $^{151}\text{Eu}$  Mössbauer spectra of flux-grown  $\text{EuCu}_2\text{Si}_2$  have led to it being identified as a spin glass [29], however neutron diffraction measurements show that at least partial long-range antiferromagnetic order occurs (Ryan et al. 2014, unpublished).

In order for moments derived from elastic neutron diffraction to be compared with hyperfine fields from  $^{151}\text{Eu}$  Mössbauer spectra, we need to bear in mind the very different nature of the two measurements. The former is sensitive only to the long-ranged magnetic order, while the latter sees any magnetic order that persists longer than the characteristic measuring time of the Mössbauer event, typically nanoseconds. In some sense, for Mössbauer spectroscopy to see a moment, that moment simply has to be “stopped” (at least for long enough to be seen), while for neutron diffraction to see a magnetic signal, the moments must be “organised”. This difference is critical. To first order, a spin glass with random isotropically frozen spins looks the same in a Mössbauer spectrum as a ferromagnet—there are significant time-averaged moments—while to neutron diffraction, a spin glass looks like a paramagnet—there is no long-ranged organisation of the magnetic structure. Contradictions between neutron-derived and Mössbauer-derived moments may originate from this very different sensitivity.

We now turn, finally, to the  $\text{EuT}_2\text{X}_2$  compound system and try to use moments, fields and isomer shifts to extend our understanding of both the transfer process and the ordering behaviour. Figure 4 shows data for a variety of silicides and germanides drawn from a compilation by Grandjean and Long [16]. Additional data on Pd-substituted  $\text{EuAu}_2\text{Si}_2$  [42] follows the trend remarkably well. There is a clear and strong correlation between  $B_{\text{hf}}$  and  $\delta$  but, as noted by Raffius et al. [43], the slope of the fitted line in Fig. 4 has the opposite sign and a magnitude that is four times larger than that shown in Fig. 1.

An immediate conclusion from the data presented in Figs. 1 and 4 is that while strong correlations can be found between  $B_{\text{hf}}$  and  $\delta$  within a well defined subset of materials, the correlation does not transfer well between systems. The *range* of values taken by  $B_{\text{hf}}$  in the isostructural  $\text{EuT}_2\text{X}_2$  systems plotted in Fig. 4 is quite remarkable. The largest field is fully 40 % larger than the smallest. The limited information on ordered moments and magnetic structures opens the possibility that some of this variation might be due to differences in the europium moments, however this is almost certainly *not* the case. Fits to high temperature susceptibility data for  $\text{Eu}(\text{Pd}_{1-x}\text{Au}_x)_2\text{Si}_2$  [42] yield effective moments that are constant, within error, for  $0.18 < x < 1.0$ . Furthermore, our neutron diffraction work on flux-grown single crystals of  $\text{EuCu}_2\text{Si}_2$  (Rowan-Weetaluktuk et al. 2014, unpublished) and arc-melted  $\text{EuCu}_2\text{Ge}_2$  [44], close to extremal examples on Fig. 4, show effectively  $7 \mu_B$  moments on the europium in both cases. Thus, while the isomer shift for  $^{151}\text{Eu}$  Mössbauer spectroscopy is a robust indicator of the europium valence, the hyperfine field

**Fig. 4** Hyperfine fields ( $B_{\text{hf}}$ ) vs. isomer shifts for a variety of  $\text{EuT}_2\text{X}_2$  compounds. Most of the *open symbols* are taken from the compilation by Grandjean and Long [16], except for those labelled “Au–Pd” which are taken from work on  $\text{Eu}(\text{Pd}_{1-x}\text{Au}_x)_2\text{Si}_2$  [42]. The *solid symbols* are taken from our (unpublished) work. The *dashed line* is a fit and has a slope of  $+5.8(4)$  T/(mm/s)

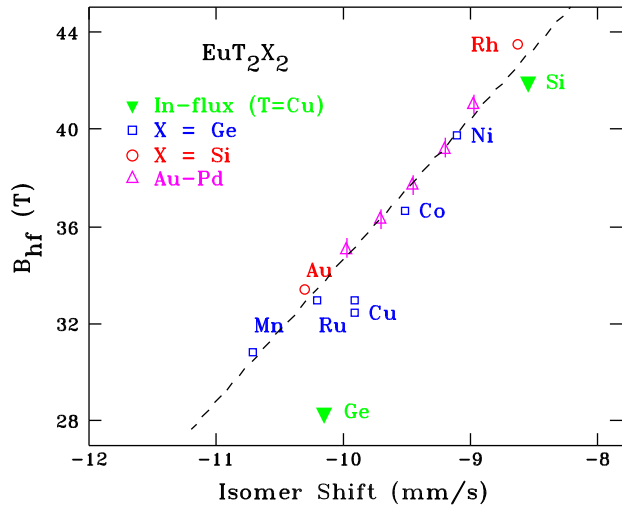
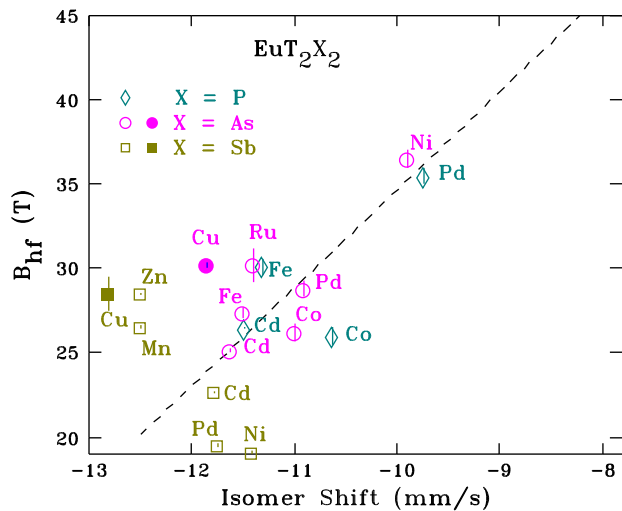


**Fig. 5** Hyperfine fields ( $B_{\text{hf}}$ ) vs. isomer shifts for a variety of  $\text{EuT}_2\text{X}_2$  compounds where X is a pnictide (P, As, Sb). Phosphides: Cd [45], Co [46, 47], Fe [46, 48, 49], Pd [50]; Arsenides: Cd [45], Co [43], Fe [51], Ni [43], Pd [43], Ru [52]; Antimonides Cd [45], Mn [53], Ni [54], Pd [55], Zn [53]. The *solid symbols* are taken from our own (unpublished) work. The *dashed line* is the same fit as used in Fig. 4 and is included for context



clearly cannot be taken as a useful measurement of the europium moment without additional information.

The indium-flux grown  $\text{EuCu}_2\text{Ge}_2$  is included on Fig. 4 as an apparent outlier but may actually support the utility of the  $B_{\text{hf}}-\delta$  correlation. If we take its position on Fig. 4 at face value, we are led to the possibility that the vertical offset from the dashed line is evidence for a smaller europium moment. Direct measurements using neutron diffraction actually yield a reduced europium moment for this material (Rowan-Weetaluktuk et al. 2014, unpublished) of  $5.0(1) \mu_B$ , while using the depression of the field from the “expected” line as an estimate of the moment reduction gives a europium moment of  $5.5(1) \mu_B$  suggesting that there may be some utility to this analysis. Within a given system, the trend may be robust enough that an outlier

may be the result of a real effect. Unfortunately, even this limited conclusion does not stand up to deeper scrutiny.

A more extensive compilation of recent work on  $\text{EuT}_2\text{X}_2$  compounds where X is a pnictide (P, As, Sb) shown in Fig. 5 suggests that the strong correlations evident in Figs. 1 and 4 may be little more than fortuitous. While some of the phosphides appear to lie close to the “expected” line, many of the new points land very far from it. Probably the biggest problem is that many of the new points lie well *above* the dashed line. There are many ways to reduce the europium moment but essentially none that would increase it above the fully stretched closed-shell value of  $7 \mu_B$ . Appeals to neighbour effects through  $B_n$  in (5) are unlikely to help. In many of the compounds used to derive the dashed line in Fig. 4, the europium is ordered in ferromagnetic sheets with the sheets above and below (along the *c*-axis) coupled antiferromagnetically. This configuration maximises the neighbour contribution. If  $B_n$  has the same sign as  $B_{\text{cp}}$  as it does in europium metal [19], or is essentially zero as it is in the  $\text{EuT}_5$  system [22], breaking up the ferromagnetic sheet structure might reduce  $B_n$  but this could only *reduce*  $B_{\text{hf}}$ , if it affected it at all.

## 5 Conclusions

While there may be excellent reasons to expect that  $B_{\text{hf}}$  would be correlated with the local moment on a magnetic species, particularly a simple closed-shell system like europium, very large variations in  $B_{\text{hf}}$  are seen that are definitely not related to variations in the local moment. Furthermore, attempts to introduce a first-order correction by invoking the isomer shift as a measure of electron density within the nuclear volume, and arguing that this is in some way a measure of the effectiveness of the moment in leading to a hyperfine field, also fail. The correlation, where it exists, can take either sign, and may owe more to limited sampling than it does to a real effect. It is clear that far more work needs to be done to understand the origins of the hyperfine field and how it is related to the local moment, bonding and atomic environments.

**Acknowledgements** DHR is supported by grants from Natural Sciences and Engineering Research Council of Canada and Fonds Québécois de la Recherche sur la Nature et les Technologies. JMC acknowledges support from the Australian Research Council and the University of New South Wales. We acknowledge assistance from W.N. Rowan-Weetaluktuk with some of the <sup>151</sup>Eu Mössbauer measurements. The  $\text{EuCu}_2\text{As}_2$  and  $\text{EuCu}_2\text{Sb}_2$  samples were provided by Prof. D.C. Johnston, Department of Physics and Astronomy, Iowa State University, and are part of an on-going neutron diffraction study.

## References

1. Stewart, G.A.: Metals Forum **18**, 177 (1994)
2. Ryan, D.H., Cadogan, J.M., Voyer, C.J., Napoletano, M., Riani, P., Cranswick, L.M.D.: Modern Phys. Lett. B **24**, 1 (2010)
3. Watson, R.E., Freeman, A.J.: Phys. Rev. **123**, 2027 (1961)
4. Ohnishi, S., Freeman, A.J., Weinert, M.: Phys. Rev. B **28**, 6741 (1983)
5. Ebert, H., Winter, H., Johnson, D.D., Pinski, F.J.: J. Phys. Condens. Matter **2**, 443 (1990)
6. Elzain, M.E., Ellis, D.E., Guenzburger, D.: Phys. Rev. B **34**, 1430 (1986)
7. Elzain, M.E.: J. Phys. Condens. Matter **3**, 2089 (1991)

8. Vincze, I., Kollár, J.: *Phys. Rev. B* **6**, 1066 (1972)
9. Dubiel, S.M.: *J. Alloys Compd.* **488**, 18 (2009)
10. Le Caer, G., Malaman, B., Venturini, G., Kim, I.B.: *Phys. Rev. B* **26**, 5085 (1982)
11. Venturini, G., Malaman, B., Le Caër, G., Fruchart, D.: *Phys. Rev. B* **35**, 7038 (1987)
12. Perry, L.K., Ryan, D.H., Venturini, G.: *Phys. Rev. B* **75**, 144417 (2007)
13. Perry, L.K., Ryan, D.H., Venturini, G.: *J. Appl. Phys.* **101**, 09K504 (2007)
14. Lee-Hone, N.R., Lemoine, P., Ryan, D.H., Malaman, B., Vernière, A., Le Caër, G.: In: ICAME 2013 Proceedings, Hyperfine Interactions (2014, submitted)
15. Cadogan, J.M., Ryan, D.H.: *J. Alloys Compd.* **326**, 166 (2001)
16. Grandjean, F., Long, G.J.: In: Long, G.J., Grandjean, F. (eds.) *Mössbauer Spectroscopy Applied to Inorganic Chemistry*, vol. 3, pp. 513–597. Plenum, New York (1989)
17. Nowik, I., Dunlap, B.D., Wernick, J.H.: *Phys. Rev. B* **8**, 238 (1973)
18. Wickman, H.H., Nowik, I., Wernick, J.H., Shirley, D.A., Frankel, R.B.: *J. Appl. Phys.* **37**, 1246 (1966)
19. Hüfner, S., Wernick, J.H.: *Phys. Rev.* **173**, 448 (1968)
20. Baker, J.M., Williams, F.I.B.: *Proc. R. Soc. Lond. A* **267**, 283 (1962)
21. Passell, L., Sailor, V.L., Schermer, R.I.: *Phys. Rev.* **135**, A1767 (1964)
22. van Steenwijk, F.J., Huiskamp, W.J., Lefever, H.T., Thiel, R.C., Buschow, K.H.J.: *Physica B+C* **86–88**, 89 (1977)
23. Bauminger, E.R., Froindlich, D., Nowik, I., Ofer, S., Felner, I., Mayer, I.: *Phys. Rev. Lett.* **30**, 1053 (1973)
24. Röhler, J., Wohlleben, D., Kaindl, G., Balster, H.: *Phys. Rev. Lett.* **49**, 65 (1982)
25. Sales, B.C., Viswanathan, R.: *J. Low Temp. Phys.* **23**, 449 (1976)
26. Scherzberg, A., Sauer, C., Köbler, U., Zinn, W., Röhler, J.: *Solid State Commun.* **49**, 1027 (1984)
27. Pagliuso, P.G., Sarrao, J.L., Thompson, J.D., Hundley, M.F., Sercheli, M.S., Urbano, R.R., Rettori, C., Fisk, Z., Oseroff, S.B.: *Phys. Rev. B* **63**, 092406 (2001)
28. Stadnik, Z.M., Wang, P., Żukrowski, J., Cho, B.K.: *Hyperfine Interact.* **169**, 1295 (2006)
29. Wang, P., Stadnik, Z.M., Żukrowski, J., Cho, B.K., Kim, J.Y.: *Phys. Rev. B* **82**, 134404 (2010)
30. Felner, I.: *J. Phys. Chem. Solids* **36**, 1063 (1975)
31. Reehuis, M., Jeitschko, W., Möller, M.H., Brown, P.J.: *J. Phys. Chem. Solids* **53**, 687 (1992)
32. Xiao, Y., Su, Y., Meven, M., Mittal, R., Kumar, C.M.N., Chatterji, T., Price, S., Persson, J., Kumar, N., Dhar, S.K., Thamizhavel, A., Brueckel, T.: *Phys. Rev. B* **80**, 174424 (2009)
33. Felner, I., Nowik, I.: *J. Phys. Chem. Solids* **39**, 767 (1978)
34. Nowik, I., Felner, I., Bauminger, E.R.: *Phys. Rev. B* **55**, 3033 (1997)
35. Hofmann, M., Campbell, S.J., Edge, A.V.J.: *Phys. Rev. B* **69**, 174432 (2004)
36. Ryan, D.H., Cranswick, L.M.D.: *J. Appl. Crystallogr.* **41**, 198 (2008)
37. Ryan, D.H., Cadogan, J.M., Cranswick, L.M.D., Gschneidner, Jr., K.A., Pecharsky, V.K., Mudryk, Y.: *Phys. Rev. B* **82**, 224405 (2010)
38. Ryan, D.H., Cadogan, J.M., Xu, S., Xu, Z., Cao, G.: *Phys. Rev. B* **83**, 132403 (2011)
39. Rhyee, J.S., Cho, B.K., Ri, H.C.: *J. Appl. Phys.* **93**, 8346 (2003)
40. Hossain, Z., Geibel, C., Yuan, H.Q., Sparn, G.: *J. Phys.: Condens. Matter* **15**, 3307 (2003)
41. Wang, P., Stadnik, Z.M., Żukrowski, J., Cho, B.K., Kim, J.Y.: *Solid State Commun.* **150**, 2168 (2010)
42. Abd-Elmeguid, M.M., Sauer, C., Köbler, U., Zinn, W.: *Z. Phys. B Condens. Matter* **60**(2–4), 239 (1985)
43. Raffius, H., Mörsen, E., Mosel, B.D., Müller-Warmuth, W., Jeitschko, W., Terbüchte, L., Vomhof, T.: *J. Phys. Chem. Solids* **54**, 135 (1993)
44. Rowan-Weetaluktuk, W.N., Ryan, D.H., Lemoine, P., Cadogan, J.M.: *J. Appl. Phys.* (2014, submitted)
45. Schellenberg, I., Pfannenschmidt, U., Eul, M., Schwickert, C., Pöttgen, R.: *Z. Anorg. Allg. Chem.* **637**, 1863 (2011)
46. Mörsen, E., Mosel, B.D., Müller-Warmuth, W., Reehuis, M., Jeitschko, W.: *J. Phys. Chem. Solids* **49**, 785 (1988)
47. Chefki, M.: Abd-Elmeguid, M.M., Micklitz, H., Huhnt, C., Schlabit, W., Reehuis, M., Jeitschko, W.: *Phys. Rev. Lett.* **80**, 802 (1998)
48. Ni, B., Abd-Elmeguid, M.M., Micklitz, H., Sanchez, J.P., Vulliet, P., Johrendt, D.: *Phys. Rev. B* **63**, 100102 (2001)
49. Feng, C., Ren, Z., Xu, S., Jiang, S., Xu, Z., Cao, G., Nowik, I., Felner, I., Matsubayashi, K., Uwatoko, Y.: *Phys. Rev. B* **82**, 094426 (2010)
50. Sampathkumaran, E.V., Perscheid, B., Kaindl, G.: *Solid State Commun.* **51**, 701 (1984)

51. Błachowski, A., Ruebenbauer, K., Żukrowski, J., Bukowski, Z., Rogacki, K., Moll, P.J.W., Karpinski, J.: *Phys. Rev. B* **84**, 174503 (2011)
52. Jiao, W.H., Felner, I., Nowik, I., Cao, G.H.: *J. Supercond. Nov. Magn.* **25**, 441 (2012)
53. Schellenberg, I., Eul, M., Hermes, W., Pöttgen, R.: *Z. Anorg. Allg. Chem.* **636**, 85 (2010)
54. Schellenberg, I., Eul, M., Pöttgen, R.: *Z. Naturforsch.* **66b**, 1179 (2011)
55. Schellenberg, I., Eul, M., Pöttgen, R.: *Z. Naturforsch.* **65b**, 18 (2010)